

Study of Heat Transfer in a Kapok Material from the Convective Heat Transfer Coefficient and the Excitation Pulse of Solicitations External Climatic

¹M. Dieng, ¹I. Diagne, ¹B. Fleur, ¹A. Kane, ¹M.L. Sow, ²F. Niang and ¹G. Sissoko
¹Faculty of Science and Technology, University Cheikh Anta Diop, Dakar, Senegal
²University Insitute of Technology IUT/UT, University of Thies, Senegal

Abstract: The aim of this study is to characterize thermal insulating local material, kapok, from a study in 3 dimensions in Cartesian coordinate and in dynamic frequency regime. From a study a 3 dimensional the heat transfer through a material made of wool kapok (thermal conductivity: $\lambda = 0.035$ W/m/K; density: $\rho = 12.35$ kg/m³; thermal diffusivity: $\alpha = 17, 1.10 \cdot 10^{-7}$ m²/s) is presented. The evolution curves of temperature versus convective heat transfer coefficient have helped highlight the importance of pulse excitation and the depth in the material. The thermal impedance is studied from representations of Nyquist and Bode diagrams allowing characterizing the thermal behavior from thermistors. The evolution of the thermal impedance with the thermal capacity of the material is presented.

Keywords: Dynamic frequency regime, heat exchange coefficient, kapok, thermal impedance, thermal insulation

INTRODUCTION

The study is part of improving the use of local natural products of the thermal insulation (Meukam *et al.*, 2004). Heat transfer through the material kapok (Voumbo *et al.*, 2010a) is studied by considering a parallelepiped-shaped material Kapok is wool taken from the fruit of a tree, kapok. This is a very light fiber characterized by its waterproof and rot-proof. These thermal properties (Jannot *et al.*, 2009) (thermal conductivity: $\lambda = 0.035$ W/m/K; thermal diffusivity: $\alpha = 17, 1.10 \cdot 10^{-7}$ m²/s) (Voumbo *et al.*, 2010b; Gaye *et al.*, 2001) make it a very good natural insulating. The material kapok behavior under stress climate is studied as a function of convective heat transfer coefficient. The dynamic thermal impedance of the material is studied from the curves of representations of Bode and Nyquist, The evolution of the thermal impedance of the material is given as a function of the heat capacity of the material.

METHODOLOGY

The heat equation is solved at 3 dimensions in rectangular coordinates (Ould Brahim, 2011):

$$\frac{\partial^2 T(x,y,z,t)}{\partial x^2} + \frac{\partial^2 T(x,y,z,t)}{\partial y^2} + \frac{\partial^2 T(x,y,z,t)}{\partial z^2} - \frac{1}{\alpha} \frac{\partial T(x,y,z,t)}{\partial t} = 0 \quad (1)$$

where,

$T(x, y, z, t)$: The temperature inside the material at a time t (sec)

α : The coefficient of thermal diffusivity (m²/s)

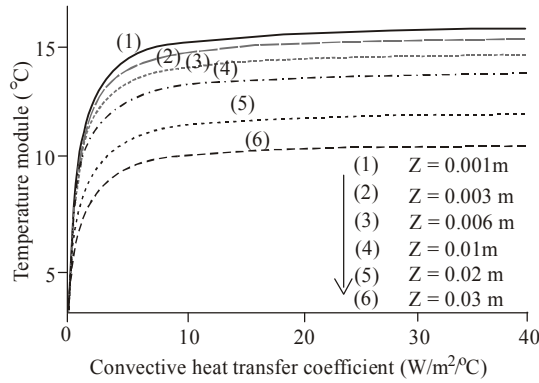
From the method of separation of variables of space and time Eq. (2) and applying the boundary conditions imposed (Ould Brahim, 2011), we obtain a solution given by Eq. (3). The heat flux density and the thermal impedance of the material are given respectively by Eq. (4) and (5):

$$T(x, y, z, t) = F(x, y, z) \cdot \psi(t) = \theta_1(x) \cdot \theta_2(y) \cdot \theta_3(z) \cdot \psi(t) \quad (2)$$

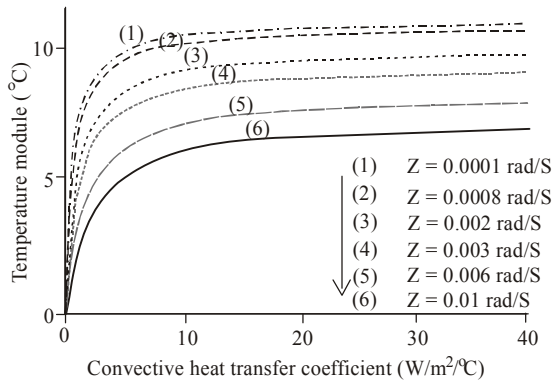
$$T(x, y, z, t) = \sum_{m=1}^{+\infty} \sum_{n=1}^{+\infty} \left\{ \begin{array}{l} \left[\cos(\beta_m x) + \frac{h_{1x}}{\lambda \beta_m} \sin(\beta_m x) \right] \times \\ \left[\cos(\gamma_n y) + \frac{h_{1y}}{\lambda \gamma_n} \sin(\gamma_n y) \right] \\ \times \left[A_{mn} \cosh(L_{mn} z) + B_{mn} \sinh(L_{mn} z) \right] \times e^{i\omega t} \end{array} \right\} \quad (3)$$

$$\vec{\Phi} = -\lambda \cdot \overrightarrow{\text{grad}T} = -\lambda \left(\frac{\partial T(x,y,z,t)}{\partial x} \vec{e}_x + \frac{\partial T(x,y,z,t)}{\partial y} \vec{e}_y + \frac{\partial T(x,y,z,t)}{\partial z} \vec{e}_z \right) \quad (4)$$

$$Z(x, y, z) = \frac{\sum_{m=1}^{+\infty} \sum_{n=1}^{+\infty} \left\{ \begin{array}{l} \left[\cos(\beta_m x) + \frac{h_{1x}}{\lambda \beta_m} \sin(\beta_m x) \right] \\ \times \left[\cos(\gamma_n y) + \frac{h_{1y}}{\lambda \gamma_n} \sin(\gamma_n y) \right] \\ \times \left[A_{mn} (1 - \cosh(L_{mn} z)) - B_{mn} \sinh(L_{mn} z) \right] \end{array} \right\} \times e^{i\omega t}}{\sqrt{\Phi_1(x,y,z,t)^2 + \Phi_2(x,y,z,t)^2 + \Phi_3(x,y,z,t)^2}} \quad (5)$$



(a)



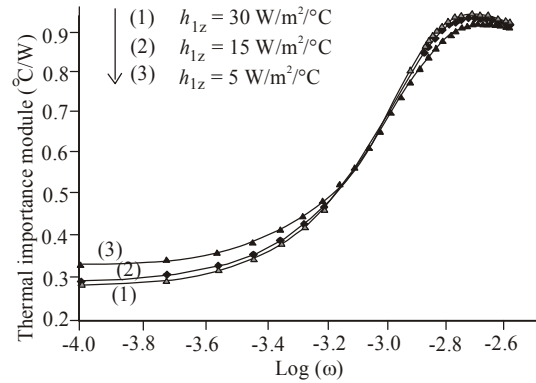
(b)

Fig. 1: Evolution of the temperature in the material depending on the coefficient of exchange to the front face of the material, a) influence of depth, b) influence of pulse excitation
 $z: 0.01 \text{ m}; x: 0.02 \text{ m}; y: 0.01 \text{ m}; \omega: 0.001 \text{ rad/S}; h_{2x}: 0.05 \text{ W/m}^2/\text{°C}$

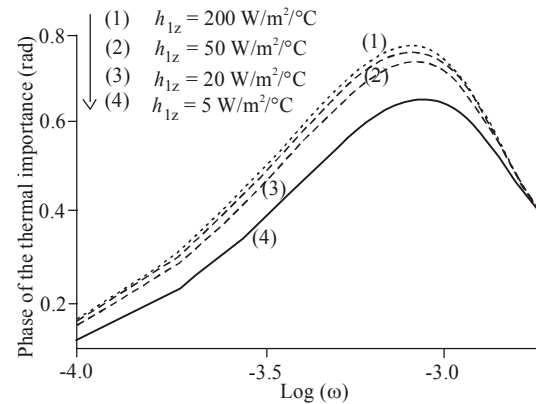
RESULTS

Temperature and heat exchange coefficient: We present in Fig. 1a and 1b-curves evolution of the temperature inside the material according to the heat exchange coefficient. We highlight the influence of the depth and the excitation pulse solicitations climate outside.

The curves show the same profile. The heat transmitted into the material increases with the the heat exchange coefficient. When the the heat exchange coefficient becomes significant, it appears a threshold value from which the temperature remains constant at a point of the material. Figure 1a shows that the amplitude of the temperature module decreases rapidly with depth of the material. The curves in Fig. 1a shows a high heat retention with increasing depth. Figure 1b shows that the temperature within the material is even more important than the angular excitation is low



(a)

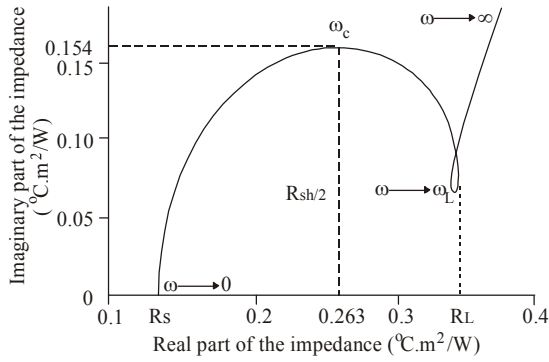


(b)

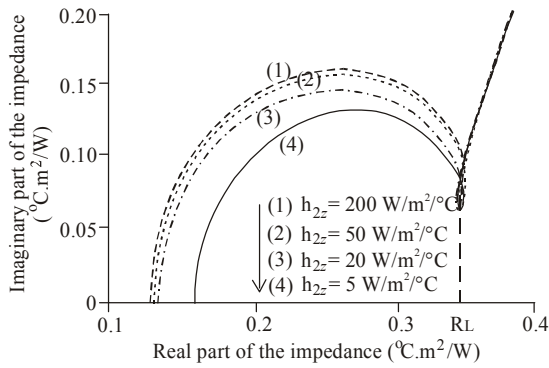
Fig. 2: Bode diagrams, a) module of the impedance, b) phase of the impedance
 $x: 0.01 \text{ m}; y: 0.001 \text{ m}; z: 0.02 \text{ m}; h_{2x}: 0.05 \text{ W/m}^2/\text{°C}$

that is to say that periods of external climatic stresses are important.

Bode diagram and representation of nyquist: Figure 2a and 2b are respectively the Bode representations of impedance and its phase. For excitatory pulses from the external environment around 10^3 rad/s , the impedance module increases significantly reflecting a sharp decrease in the density of heat flux within the material. The low frequencies present a low impedance module and practically constant favoring a strong heat transfer in accordance with the temperature curves (Fig. 1). The modulus of the impedance for low frequencies corresponds to the series resistance R_s (Fig. 3), the series resistance values depending on the heat exchange coefficient is given in Table 1. For high frequencies, the modulus of the thermal impedance approaches a thermal resistance that is the sum of the series resistance and thermal resistance.



(a)



(b)

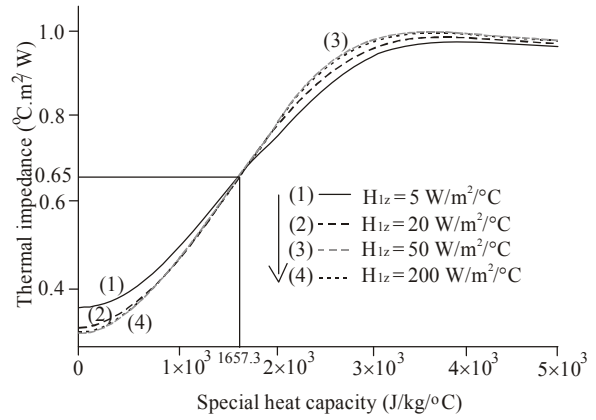
Fig. 3: Nyquist representations a) method for determining electrical parameters b) influences of convective heat transfer coefficient
 x: 0.01 m; y: 0.001 m; z: 0.02 m; h_{2x} : 0.05 W/m²/°C

Table 1: Values of the series resistor and shunt resistance of the kapok material according to the heat exchange coefficient h_{1z} ; $h_{2z} = 0.05 \text{ W/m}^2/\text{°C}$

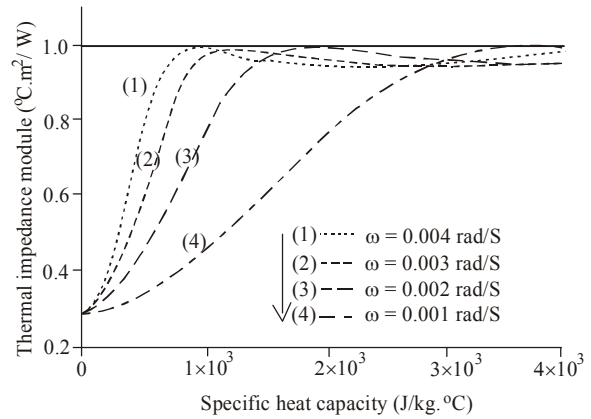
| $h_{1z} (\text{W/m}^2/\text{°C})$ | 5 | 20 | 50 | 200 |
|-------------------------------------|-------|-------|-------|-------|
| R_s | 0.160 | 0.138 | 0.132 | 0.129 |
| $R_s + R_{sh}$ | 0.700 | 0.664 | 0.654 | 0.649 |
| R_{sh} | 0.540 | 0.526 | 0.522 | 0.520 |
| $R_L (\omega \rightarrow \omega_L)$ | 0.344 | 0.344 | 0.344 | 0.344 |

The Fig. 2b shows that the material stores heat by capacitive and inductive effects coupled with a predominance of inductive effects.

Heat capacity and thermal impedance: The Fig. 4a and b show the evolution of the thermal impedance as a function of the heat capacity of the material. The Fig. 4a shown that for relatively low thermal capacity, increasing the heat exchange coefficient corresponds to a decrease in the thermal impedance module, resulting in bad behavior in thermal insulation. When the heat capacity becomes large, the thermal impedance



(a)



(b)

Fig. 4: Module of the thermal impedance of the material kapok depending on the specific heat a) influence of heat exchange coefficient to the front face, b) influence of the exciter pulse
 x: 0.02 m; y: 0.01 m; z: 0.01 m; h_{2x} : 0.05 W/m²/°C; t: 1 heure

Table 2: Comparison of the maximum values of the modulus of the thermal impedance of the material with the heat exchange coefficient of the front face of the material and its heat capacity

| $h_{1z} (\text{W/m}^2/\text{°C})$ | 200 | 50 | 20 | 5 |
|-----------------------------------|-------|-------|-------|-------|
| $C (\text{J/Kg}/\text{°C})$ | 3620 | 3665 | 3785 | 4215 |
| $IZI (\text{°C.m}^2/\text{W})$ | 0.995 | 0.992 | 0.987 | 0.970 |

Table 3: Comparison of maximum values of the modulus of the thermal impedance of the material with the excitation pulse and the specific heat of the material

| $\omega (\text{rad/S})$ | 0.004 | 0.003 | 0.002 | 0.001 |
|--------------------------------|-------|-------|-------|-------|
| $C (\text{J/Kg}/\text{°C})$ | 945 | 1265 | 1905 | 3765 |
| $IZI (\text{°C.m}^2/\text{W})$ | 0.989 | 0.989 | 0.989 | 0.989 |

becomes significant which results in a good thermal insulator behavior. The modulus of the impedance

increases so with the heat exchange coefficient. The Fig. 4a shows the existence of an optimal capacity $C = 1657 \text{ J/kg/}^\circ\text{C}$ thus constituting a reversal point.

The Fig. 4b shows that for low thermal capacity, the influence of the external pulse is practically zero. When the capacity becomes large, the impedance module increases with the outer exciter pulse. The curves show maxima and a reversal of the phenomenon observed for large thermal capacity (Table 2 and 3). Note that the dulus of the impedance remains practically constant around a mean value (Table 2 and 3).

CONCLUSION

The study showed the important qualities of thermal insulating of material kapok. The spectroscopic study of the impedance from the representations of Nyquist and Bode plots were used to analyze the phenomena of heat retention.

The study of the impedance from the thermal capacity of the material allowed highlighting the existence of an optimal thermal insulation capacity depending on the characteristics of surrounding environments: external pulse excitation and heat transfer coefficient convective.

REFERENCES

- Gaye, S., F. Niang, I.K. Cissé, M. Adj, G. Menguy and G. Sissoko, 2001. Characterisation of thermal and mechanical properties of polymer concrete recycled. *J. Sci.*, 1(1): 53-66.
- Jannot, Y., A. Degiovanni and G. Payet, 2009. Thermal conductivity measurement of insulating materials with a 3 layers device. *Int. J. Heat Mass Tran.*, 52: 1105-1111.
- Meukam, P., Y. Jannot, A. Noumow and T.C. Kofan, 2004. Thermo physical characteristics of economical building materials. *Constr. Build. Mater.*, 18: 437-443.
- Ould Brahim, M.S., I. Diagne, S. Tamba, F. Niang and G. Sissoko, 2011. Characterization of the minimum effective layer of thermal insulation material tow-plaster from the method of thermal impedance. *Res. J. Appl. Sci. Eng. Technol.*, 3(4): 337-343.
- Voumbo, M.L., A. Wareme, S. Gaye, M. Adj and G. Sissoko, 2010a. Characterization of the thermophysical properties of kapok. *Res. J. Appl. Sci. Eng. Technol.*, 2(2): 143-148.
- Voumbo, M.L., A. Wareme and G. Sissoko, 2010b. Characterization of local insulators: Sawdust and wool of kapok. *Res. J. Appl. Sci. Eng. Technol.*, 2(2): 138-142.